NASA
Technical
Paper
2132

AUGUST 1983

Modeling Interface Motion of Combustion (MIMOC)

A Computer Code for Two-Dimensional, Unsteady Turbulent Combustion

Ahmed F. Ghoniem,
Cecil J. Marek, and
Antoni K. Oppenheim

NASA

25th Anniversary
1958-1983

NASA
Technical
Paper
2132

1983

Modeling Interface Motion of Combustion (MIMOC)

A Computer Code for Two-Dimensional, Unsteady Turbulent Combustion

Ahmed F. Ghoniem
University of California, Berkeley
Berkeley, California

Cecil J. Marek
Lewis Research Center
Cleveland, Ohio

Antoni K. Oppenheim
University of California, Berkeley
Berkeley, California

NASA
National Aeronautics
and Space Administration

**Scientific and Technical
Information Branch**

1983

Summary

This report describes a computer program for calculating the flow field and flame propagation in a turbulent combustion tunnel. The program employs an algorithm for turbulent combustion modeling described by Ghoniem, Chorin, and Oppenheim (refs. 1 and 2). It uses the random vortex method of Chorin (ref. 3), which has the advantage of allowing the turbulent field to evolve as a fundamental solution of the Navier-Stokes equations without averaging or closure modeling. The flame front, which is treated as an interface between the reactants and the products, is computed by using an algorithm developed by Chorin (ref. 4) and exploiting a technique by Noh and Woodward (ref. 5) for simple line interface calculation. The flow is treated as "slightly compressible." This allows for the increase in specific volume in the course of combustion to modify the flow field without any acoustic effects in order to model the effect of significant changes in density that occur at relatively low Mach numbers.

The program provides numerical and graphical information about the vorticity field, the flame front location, and the composition profiles expressed in terms of the ratio of reactants to products, all as time-evolving fields. These data can be used to obtain average and stationary statistics of the turbulent field. In addition, overall performance parameters like the turbulent flame speed and the reattachment length behind a rearward-facing step in a channel can be deduced from these data.

The program is rendered some flexibility by making most of its operation essentially independent of the geometry of the enclosure containing the flow field. Although most calculations are carried out in a universal transformed plane, the description of the geometry of the channel is restricted to a group of subroutines in order to allow a variety of configurations to be treated with a minimum of modifications. In this report the geometry of a channel with a rearward-facing step of an arbitrary height is used as an example.

Introduction

Turbulent combustion involves a complex set of interactions between essentially unstable fluid flow phenomena and transient exothermic chemical reactions that produce a significant increase in the specific volume of the flowing mixture. In general, these interactions influence the structure of the flow field as well as the progress of chemical processes and lead to a highly untractable situation, especially when basic mechanisms of both phenomena represent substantial challenges in their analyses.

On one hand, chemical heat release, accompanied by large and rapid changes in specific volume, results in high flow acceleration that modifies and augments the turbulent field. It has been experimentally shown that when flame advection by the flow field is significantly larger than flame advancement due to normal burning speed, different rates of energy release can trigger different modes of instability and turbulent eddy interaction in the flow field according to Keller et al. (ref. 6). On the other hand, combustion fronts are essentially convected by the flow field, and their geometries are determined by the flow field structure. Thus overall reaction rates, controlled by mixing hot products and cold reactants, are strongly influenced by the turbulent field. The closed loop of interaction thus formed between turbulence and combustion makes it necessary for models of these processes to take their mutual influence clearly into account. Mellor (ref. 7) and Mellor and Ferguson (ref. 8) demonstrate that this complex interaction hinders numerical models from reproducing experimental data; Bray (refs. 9 and 10) points out the difficulties of accurately incorporating such interactions into computational schemes.

In principle, the problem can be described in terms of a set of conservation equations coupled with a chemical kinetic scheme for a particular reaction as shown, for example, by Williams (ref. 11). In many practical situations one cannot expect a viable solution for this system of equations since they are highly nonlinear and intrinsically unstable and their fundamental solutions vary over a wide range of time scales. Moreover, in most cases of interest the equations are elliptic, with recirculating fields and sharp gradients in the solution domain, and thus contain a wide spectrum of length scales.

Both the initial and boundary conditions are statistical, and the solutions are expected to be very sensitive to small perturbations in these conditions according to Libby and Williams (ref. 12). The effect of these perturbations cannot be played down. In fact, instabilities introduced in the flow field by the growth of perturbations can, paradoxically enough, enhance the stability of turbulent flames. This has been demonstrated by the numerical analysis developed in reference 2 to model the fluid mechanical phenomena of turbulent flow in a combustion tunnel.

The model presented herein establishes the link between turbulence and combustion in terms of the primary dynamic variable: the velocity field. Turbulence is solved from first principles in terms of the dynamics of the vorticity field by using the random vortex method. The random vortex method computes the vorticity field as an equivalent number of discrete elements, called vortex blobs. The interaction of the vortex blobs is determined, and they are moved with each time step. Diffusion is represented by the random walk of the blobs.

This method neither imposes an averaging procedure, which in turn requires closure modeling, nor introduces extra numerical diffusion into the solution, which can dampen the inherent natural instabilities of the flow field. Thus it can reproduce detailed turbulent eddy interactions in rapidly changing fields. The mechanical effects of combustion are modeled by the motion of the flame front, which is composed of advection and normal propagation as a laminar flame, as well as by a distribution of volumetric sources inside the combustion zone that introduces the effect of combustion exothermicity into the velocity field. The linkage between turbulence and combustion in this model provides the mechanism through which the interaction between the two fields evolves with time and spreads throughout the field. Thus the algorithm is particularly useful for the study of such phenomena as inflammation, flame instabilities, and transient flow fields occurring in internal combustion engines.

The report is divided into three sections: the model, the algorithm, and the program. Under the model the equations used in formulating the problem are presented along with an overall outline of the solution steps. Under the algorithm the solution procedures are described in detail and the formulas used to implement each step are given. Under the program the organization of various subroutines in the code, as well as the function of each, is presented. The computer program, which is available from COSMIC, University of Georgia, Athens, Ga. 30602, contains an extensive list of variable definitions and comments on major steps to make it readily understandable. Examples of computer graphics motion pictures of the vorticity field and the flame front interface are presented in film supplement C-308, which is available on loan and described at the back of this report.

The authors are grateful to Professor Alexandre J. Chorin for his help and advice throughout the course of this work. He also provided the original code of the flame propagation algorithm. Mr. Youwei Dai produced part of the computations presented in this report.

Symbols

d	influence factor of vortex sheet
F	differential transformation function, $d\zeta/dz$
f	fractional volume of burned medium in cell
H_1	height of incoming flow channel
H_2	height of main flow channel
h	length of vortex sheet
h_c	side length of cell
i	$\sqrt{-1}$
N_S	number of source blobs
N_V	number of vortex blobs
$\mathbf{n}$	surface normal vector
R	Reynolds number
$\mathbf{r}$	position vector, x,y
S	burning speed
S_u	normal burning speed
t	time
Δt	time step
Δt_c	combustion time step
u	velocity in x direction
$\mathbf{u}$	velocity vector in physical plane, u,v
v	velocity in y direction
w	complex velocity, $u-iv$
x,y	Cartesian space coordinates
z	complex coordinate in physical plane, $x+iy$
α	expansion ratio, H_2/H_1
Γ	circulation of vortex blob
γ	circulation per unit length of vortex sheet
Δ	source blob strength
δ	thickness of sheet layer
ϵ	volume source strength
ζ	complex vector in transformed plane
η	Gaussian random number
μ	dynamic viscosity of fresh mixture
ν	specific volume ratio across flame
ξ	vorticity
ρ	density of fresh mixture
ρ_0	blob core radius

Subscripts:

b	burned medium
c	combustion
f	flame front
i,j	for i^{th} blob summed over all other j blobs
s	source velocity
v	vortex velocity
ϵ	produced by combustion
δ	evaluated at edge of vortex sheet
ξ	produced by turbulence
0	reference point
∞	incoming flow

Superscripts:

$\sim$	complex conjugate
*	sheet property

The Model

The analytical model is described schematically by the block diagram shown in figure 1. Each block contains either the relevant equations used to model a physical process or the link between two subsequent processes. The diagram is constructed of two loops that are linked together by the total velocity field **u**. The loop on the left side shows how vortex dynamics is applied to solve the turbulent field by the random vortex method (refs. 3, 13, and 14). The key element in this loop is the vorticity ξ, which is treated as a set of discrete elements that are transported by convection due to the total velocity field **u** and by diffusion expressed in terms of a random walk. Vorticity is created on solid boundaries to satisfy the no-slip condition and produces the solenoidal part of the velocity field $\mathbf{u}_\xi$.

The loop on the right side of figure 1 illustrates how combustion is incorporated into the model. The flame front, at locations specified by the vector $\mathbf{r}_f$, is treated locally as an interface between two incompressible media: the reactants and the products. The front is advected by the total velocity field **u** and propagates in the direction normal to its surface at a prescribed normal burning speed S_u. The location of the interface, as well as its displacement, is calculated by using an algorithm that utilizes the concentration field scalar f, which is defined as the local fractional volume of burned gas (ref. 4), to describe the composition field. The scalar field f is determined for a grid located in the flow. The changes in f due to burning are employed to evaluate the specific volume source strength ϵ, which is the key element of the combustion algorithm loop. These sources produce the irrotational part of the velocity field **u**.

A typical graphical output that shows various computational elements is presented in figure 2. The dots on the tails of the lines represent the positions of the vortex blobs, and the length and direction of the lines represent the magnitude and direction of the velocity. The dashes represent the edge of the flame.

The algorithm is unsteady and forward marching in time. The solution procedure is as follows:

(1) Start with potential flow
(2) Add turbulence at wall (vortex sheets)
(3) Do random walk
(4) Find flame
(5) Move with flow
(6) Move with laminar flame speed
(7) Repeat, starting with step (2)

Steps (1) to (3) are flow calculations; steps (4) to (6) are flame calculations. The solution is begun at $t = 0$. There is potential flow throughout the channel except on the boundaries where vortex sheets are added to satisfy the no-slip condition. The flow calculations are performed first and then the flame calculations. Computations

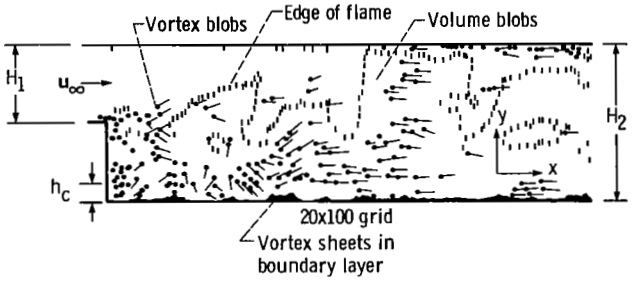

Figure 2. - Graphical output of MIMOC.

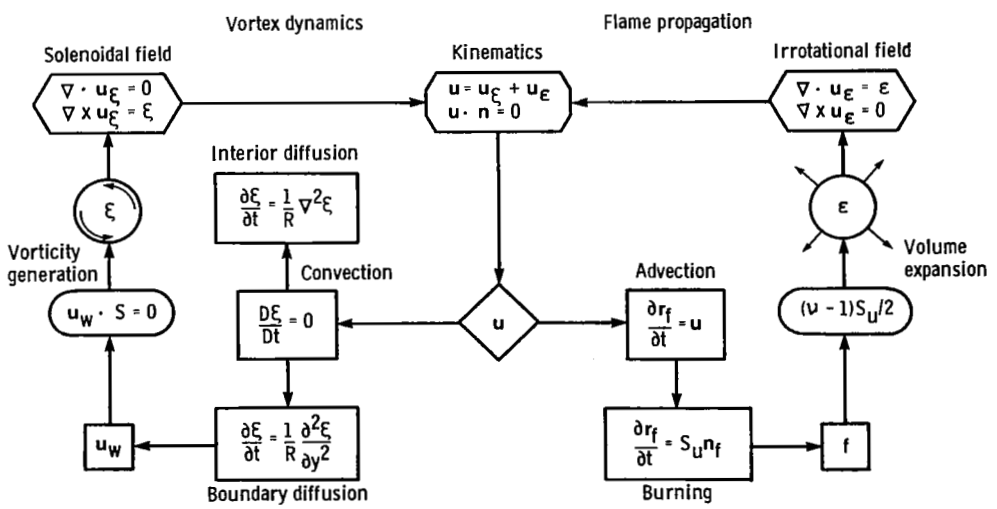

Figure 1. - Structure of MIMOC algorithm.

continue until enough iterations are reached to obtain steady statistics.

To calculate the vortex dynamics, the flow field is partitioned into a core, which represents the interior region of the flow field, where vortex blobs are located, and a numerical boundary layer, or several of them if more than one wall is considered, where vortex sheets are located. The different operations of the random vortex method and the relationship between the two kinds of vortex elements, namely vortex sheets and vortex blobs, are described next.

Each boundary layer extends over a very small distance δ, normal to the wall, in the order of magnitude $\sqrt{2\,\Delta t/R}$, where Δt is the time step and R is the Reynolds number. Within a boundary layer, vortex elements, generated on the wall to satisfy the no-slip boundary condition, are discretized along the wall direction into vortex sheets with a finite length h. The influence of these vortex sheets is restricted locally to a domain normal to their direction, the wall direction, and their diffusion is taken only normal to the wall. These elements provide a fine resolution in the near-wall region, and they satisfy the conservation of vorticity by virtue of their reflective properties (ref. 13). Their use also significantly reduces computational time as a consequence of their confined local influence in regions of high vorticity concentration.

In the interior, vortex elements become vortex blobs as they diffuse out from numerical boundary layers. The induced velocity field of a vortex blob is fully symmetric although the blob movement by diffusion is completely unbiased. The transition between sheets and blobs is smoothly maintained in the solution of the vorticity transport equation by providing a region of overlap of the two elements to allow one element to transform to another while it maintains the value of its circulation and identity. The continuity of the velocity field is maintained by extending the velocity induced by vortex blobs into the vortex sheet region.

Because the combustion model is based on the assumption of fast chemistry similar to Williams (ref. 15), either the reactants or the products may exist at the same place with an infinitely thin interface separating them. The conversion of one component of the mixture into the other is controlled by the combined effect of two factors: (1) the normal burning speed S_u, which accounts for molecular diffusion processes as well as chemical reaction kinetics, and (2) the kinematics of the interface, governed by the distribution of the concentration field $f(\mathbf{r})$. Besides, the interface is transported, or advected, by the flow field while it modifies that field by the velocity produced because of the volumetric expansion across the flame.

The concentration field is used as a way of digitizing the geometry of the flame. The plane is divided into a number of square cells by using a grid of a fixed mesh size, and f is given a value in each of these cells to describe the mixture distribution. The interface inside a cell is treated as a simple straight line whose location is determined by the value of f. Its orientation as either a horizontal or a vertical line depends on the value of f in the cell and its four neighboring cells. This technique is described in more detail in the next section. The motion of the interface line is determined by its speed, and the concomitant displacement of the fluid on both sides is used to change the value of f in the cells on both sides. When the direction of the speed is not known, like the propagation of the flame normal to itself, the scheme suggested by Chorin (ref. 4) is applied. According to Chorin, the advancement of the flame due to burning can be evaluated by Huygen's principle on recognizing that its front, propagating in the direction normal to its surface, forms an envelope to its displacement in all possible directions.

By applying the continuity requirements reference 2 used this algorithm to calculate the amount of reactants converted into products at each time step and consequently the volumetric change of the flow field due to combustion. This change gives rise to an irrotational velocity field, according to Batchelor (ref. 16) and Chorin and Marsden (ref. 17), which is added to the vortex velocity field to furnish a complete solution of the turbulent combustion system under investigation.

The Algorithm

A pragmatic description of the algorithm is presented in this section. It includes all of the formulas used for the computations but does not provide their derivation. The details of the theoretical background can be found in reference 2. All quantities used in the program are nondimensionalized with respect to the reference parameters. Length is normalized with respect to the height of the main channel H_2. Velocities are normalized with respect to the incoming flow velocity $\mathbf{u}_\infty$, and time is normalized with respect to $H_\infty/\mathbf{u}_\infty$. Thus the Reynolds number is defined as $\rho\mathbf{u}_\infty H_2/\mu$, where ρ is the fresh mixture density and μ is its dynamic viscosity.

The computational algorithm is divided into two sections: computations of vortex dynamics and computations of combustion. In the first section, vortex elements in the interior of the flow, called vortex blobs, are moved in both the physical z-plane and the transformed upper-half ζ plane. The transformation is accomplished by the general Schwarz-Christoffel transformation, which allows the solution to be mapped into a variety of physical geometries. This technique results in a computer program with most of the subroutines being geometry independent. The transformed plane is used to facilitate the computations of a velocity field with a zero

normal component along the boundaries. Vortex blobs are propelled with their own induced velocity as well as with the velocity field imposed by both the incoming potential flow and the volumetric source blobs.

The physical plane and the transformed plane for a channel with a rearward-facing step are shown in figure 3. The positions of vortex elements on the boundary walls, called vortex sheets, are then updated after calculating the velocities of the sheets from the velocity field imposed on them by the interior field. If the no-slip condition on the walls is not satisfied, new sheets are created and added to the existing vorticity field. In the second section of the algorithm, combustion calculations are performed by advancing the flame in two fractional computational steps. In the first fractional step the flame is advected by the velocity field; in the second step it is displaced by the normal burning speed of the corresponding laminar flame in order to account for combustion. The strength of volumetric sources is computed according to the combined effect of the burning speed and the specific volume ratio across the flame. Their location is established by the position of the flame front.

Computations of Vortex Dynamics

The computations start at time $t=0$, with the flow field produced by the incoming potential flow only. The tangential velocity produced by this flow along the solid walls is computed and used to produce the first vortex sheet in the field, with the proper strength to cancel this velocity. The vortex sheet is divided into a number of sheets of length h along each wall, and each of them is subdivided into a stack of smaller sheets normal to that wall. The diffusion of these stacks away from the walls and into the interior field is the source of vorticity in the flow during the course of the computations.

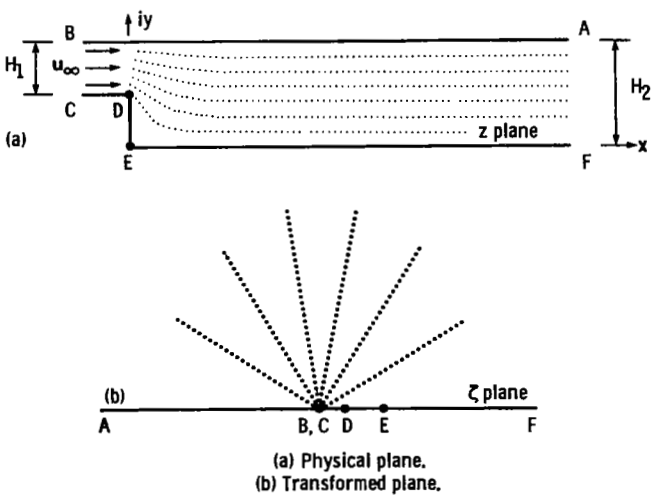

(a) Physical plane.
(b) Transformed plane.

Figure 3. - Geometry of physical and transformed planes.

The computation for each new time step, $t+\Delta t$, starts by updating the vorticity field $\xi(x,y)$. This is accomplished in two steps: (1) translation of the vorticity field, and (2) augmentation of the vorticity field. The computation of each step is presented in detail.

Translation of vorticity field. – New coordinates of each vortex blob are calculated from

$$z(t+\Delta t)=z(t)+\mathbf{u}\,\Delta t+\eta \tag{1}$$

where $z=x+iy$ is the complex coordinate of the center of a vortex blob in the z plane, $\mathbf{u}=u+iv$ is the velocity in the complex plane, and $\eta=\eta_x+i\eta_y$ is the two-dimensional random walk modeling the diffusion of vorticity of which each component is computed as a Gaussian random number with zero mean and variance $2\,\Delta t/R$. (For more details about modeling diffusion by random walk, see Ghoniem and Oppenheim, ref. 18.)

The total velocity in the z plane is evaluated by first calculating the velocity in the ζ plane as a result of the following effects:

(1) Incoming flow w_i

(2) Vortex blobs and their images, the latter to satisfy the zero normal velocity condition along the solid walls, w_v

(3) Source blobs and their images, the latter to cancel their induced normal velocity along solid boundaries, w_s

The value of the velocity, expressed in terms of a complex velocity, can be written as

$$w(\zeta)=w_i(\zeta)+\sum_{j=1}^{N_V} w_v(\zeta,\zeta_j)+\sum_{j=1}^{N_S} w_s(\zeta,\zeta_j) \tag{2}$$

where

$$w_i(\zeta)=\frac{1}{\pi\zeta} \tag{3}$$

The velocity field induced by each individual blob, evaluated as the fundamental solution of the solenoidal field and irrotational field equations shown on the top corners of figure 1, is given by

$$w_v(\zeta,\zeta_j)=-i\Gamma_j\frac{|\zeta-\zeta_j|}{2\pi\,\mathrm{Max}[|\zeta-\zeta_j|,\rho_0](\zeta-\zeta_j)}$$

$$+i\Gamma_j\frac{|\zeta-\tilde{\zeta}_j|}{2\pi\,\mathrm{Max}[|\zeta-\tilde{\zeta}_j|,\rho_0](\zeta-\tilde{\zeta}_j)} \tag{4}$$

for a vortex blob and by

$$w_s(\zeta,\zeta_j)=\Delta_j\frac{|\zeta-\zeta_j|}{2\pi\ \mathrm{Max}[|\zeta-\zeta_j|,\rho_0](\zeta-\zeta_j)}$$

$$-i\Delta_j\frac{|\zeta-\tilde{\zeta}_j|}{2\pi\ \mathrm{Max}[|\zeta-\tilde{\zeta}_j|,\rho_0](\zeta-\tilde{\zeta}_j)} \qquad (5)$$

for a source blob. In these equations, ζ is the coordinate in the transformed ζ plane, $\tilde{\zeta}=\mathrm{conj}(\zeta)$, Γ_j is the circulation of a vortex blob, N_V is the total number of vortex blobs, Δ_j is the strength of a volumetric source blob, N_S is the total number of source blobs, and ρ_0 is the radius of the blob core. The absolute value of the vortex-induced velocity inside this core is taken as a constant. The radius of the core in the ζ plane is calculated by using the transformation

$$\rho_0(\zeta_j)=\rho_0|F(\zeta_j)| \qquad (6)$$

where $\rho_0=h/\pi$ is the radius of the blob core in the z plane and h is the length of the vortex sheet. The function $F(\zeta)$, the differential transformation that maps the z plane into the ζ plane, is defined as

$$F(\zeta)=\frac{d\zeta}{dz} \qquad (7)$$

where z is nondimensionalized with respect to the channel height. The function F used for the rearward-facing step with an expansion ratio α is

$$F(\zeta)=\pi\zeta\left(\frac{\zeta-\alpha 2}{\zeta-1}\right)^{1/2}$$

The velocity in the z plane is then obtained by the inverse transformation

$$w(z)=w(\zeta)F(\zeta) \qquad (8)$$

and $\mathbf{u}=\mathrm{conj}[w(z)]$.

Because some vortex blobs may move into the boundary layers, the vorticity between the interior and the various boundaries must be resorted to make sure that the contribution of a vortex element is correctly taken into account in the next steps. The location of vortex blobs in the ζ plane is required in the next time step in order to calculate their induced velocity according to the above procedure. The location is obtained by applying the following formula:

$$\zeta(t+\Delta t)=\zeta(t)+\int_{\Delta z}F(\zeta)\,dz \qquad (9)$$

where $\Delta z=z(t+\Delta t)-z(t)$. The integration from the z plane to the ζ plane is performed by using a fourth-order Runge-Kutta method.

Augmentation of vorticity field. – Additional vortex blobs appear in the interior field as a result of vortex sheets moving outside their numerical boundary layers, as shown in figure 4. These sheets are originally generated on the wall to cancel the tangential velocity on it. Outside a layer in the order of magnitude of the variance of the random walk, vortex sheets become vortex blobs with the same circulation in order to satisfy the conservation of the total circulation. Since vortex sheets can be reflected back into the field if they move outside it, as shown by Chorin (ref. 13), this layer helps to reduce the possibility of losing vortex blobs.

To compute the position of vortex sheets, to transform sheets into blobs when necessary, and to generate new sheets on the walls, the following steps are taken for each wall:

(1) The velocity produced by the interior field u_δ is computed on the walls.

(2) The velocity is transformed into the wall coordinate system in which the wall is taken as the x axis and the normal to it as the y axis. This transformation is necessary to keep the calculations of vortex sheets independent of the wall orientation.

(3) Vortex sheets on the wall are moved according to the formula

$$z_i(t+\Delta t)=z_i(t)+\tilde{u}_i\,\Delta t+\eta_y \qquad (10)$$

where $\tilde{u}_i=u_i+iv_i$ and

$$u_i=u_{\delta_i}-0.5\,\gamma_i-\sum_{y_i}^{\delta}\gamma_i\,d_j \qquad (11)$$

Here u_{δ_i} is the velocity, calculated at x_i, at the edge of the sheet layer produced by the interior field, γ_i is the circulation per unit length of the sheet, and d_j is the influence factor defined as

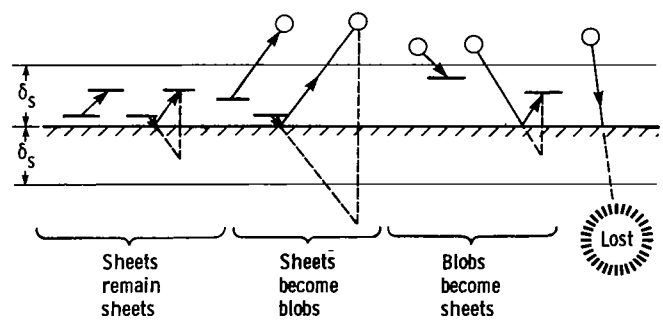

Figure 4. - Transformation of vortex elements near a solid wall between sheets and blobs.

$$d_j = 1 - \frac{|x_i - x_j|}{h}$$

The summation is taken over all of the sheets that satisfy the following conditions:

$$y_i > y_j$$

$$1 \geq d_j > 0$$

Figure 5 provides a graphical interpretation of equation (11), where the zone of influence of a vortex sheet is marked by its shadow. The normal-to-the wall velocity component is

$$v_i = \frac{I^- - I^+}{h} \tag{12}$$

where

$$I^{\pm} = u_\delta\left(x_i \pm \frac{h}{2}\right) - \sum_{y=0}^{\delta} y_j^* \gamma_j d_j^{\pm}$$

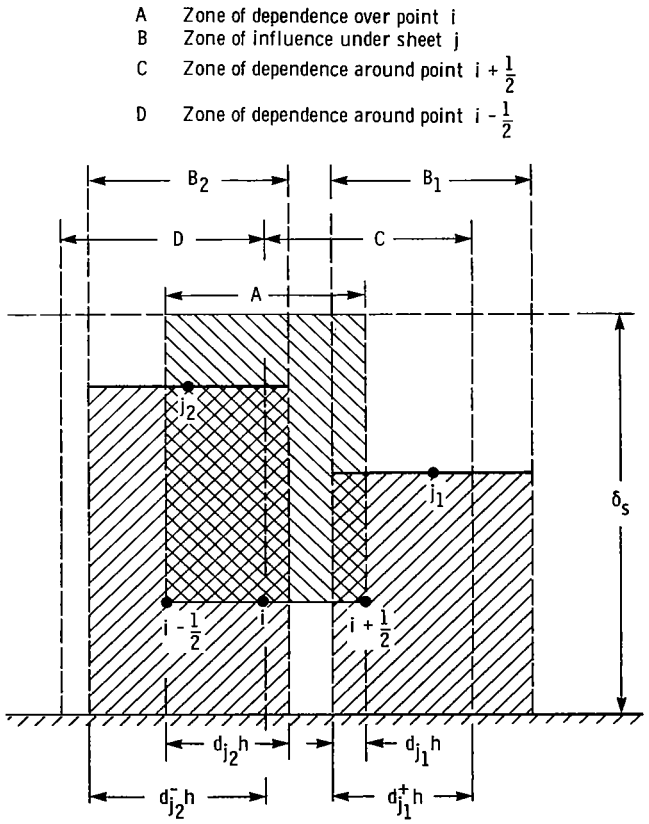

Figure 5. - Geometry showing influence of vortex sheet layer

and

$$d_j^{\pm} = 1 - \frac{|x_i \pm (h/2) - x_j|}{h}$$

The summation is taken over all of the sheets for which $0 < d_j \leq 1$, and

$$y_j^* = \text{Min}(y_i, y_j)$$

The y coordinate of the new location is checked for negative values; if $y_i < 0$, the sheet is reflected back with $y_i = -y_i$.

(4) The tangential velocity on the wall is computed by using a special case of equation (11). If $y_i = 0$,

$$u_{w_i} = y_\delta(x_i) - \sum_{y=0}^{\delta} \gamma_j d_j \tag{13}$$

If $|u_{w_i} h| \geq \Gamma_{\min}$, where $\Gamma_{\min}$ is an assigned value for the minimum circulation of a new vortex element, the appropriate number of vortex sheets are generated or removed on the wall. The numerical choice of these parameters is discussed in a later section.

(5) Finally, the coordinates of all of the vortex sheets are checked for $y > \delta$, where δ is the thickness of the numerical boundary layer. Vortex sheets that leave this layer are converted into vortex blobs in the interior field. Their coordinates are transformed back into physical coordinates and their locations in the ζ plane are calculated by using the appropriate modification of equation (9)

$$\zeta = \zeta_0 + \int_{z_0}^{z} F(\zeta) dz \tag{14}$$

where z_0 represents a reference point with a predefined transformation ζ_0. The analytical transformation that is used to evaluate z_0 from ζ_0 is

$$z = \frac{1}{\pi}\left(\log\frac{1+\alpha_\zeta}{1-\alpha_\zeta} - \frac{1}{\alpha}\log\frac{\alpha+\alpha_\zeta}{\alpha-\alpha_\zeta}\right) \tag{15}$$

where

$$\alpha_\zeta = \left(\frac{\alpha^2 - \zeta}{1-\zeta}\right)^{1/2} \tag{16}$$

Computations of Combustion

The computations of combustion consist of two components: (1) flame advancement, and (2) dynamic

effects of combustion due to volumetric expansion. The flame motion is composed of advection and combustion. They are taken into account by fractional steps as follows.

Advection. – A grid is first constructed in the physical plane to keep track of the volumetric concentration of products f in the combustion zone. The grid divides the plane into a number of cells of size h_c, as shown in figure 2. So that the advection velocity can be calculated on the grid, the centers of these cells are transformed onto the ζ plane by using equation (14). Equations (2) to (5) are applied in each step to evaluate the velocity at these centers, which is then linearly interpolated to compute the velocity component required on the sides of the cells, as shown in figure 6(a).

The orientation of the interface inside a cell is determined by comparing the value of f in the cell and its value at the four neighboring cells. If $f=0$ or $f=1$, the cell is filled with reactants or products, respectively, and no computations are required in this cell. If $0<f<1$, the interface is constructed as one of the following possibilities:

(1) Vertical neck:

$f_{i-1,j}=0$

and

$f_{i+1,j}=0$

(2) Horizontal interface:

$f_{i-1,j}>0$

and

$f_{i+1,j}>0$

(3) Vertical interface:

$f_{i-1,j}>0$

$f_{i+1,j}=0$

$f_{i,j+1}>0$

and

$f_{i,j-1}>0$

(4) Corner:

$f_{i-1,j}>0$

$f_{i+1,j}=0$

$f_{i,j-1}>0$

and

$f_{i,j+1}=0$

Figure 6(b) shows the geometrical interpretation of these arrangements. To simplify the computations, motion in two directions is split into two fractional steps, each in one dimension.

After the interface is located, its velocity is evaluated by interpolating between the velocities on both sides of the cell. The interface velocity is used to move the interface. The fluid on both of its sides is displaced in or out of the surrounding cells to accommodate this motion.

Combustion. – The motion of the flame in the direction normal to itself due to combustion is calculated in the exact manner as advection but by using the normal

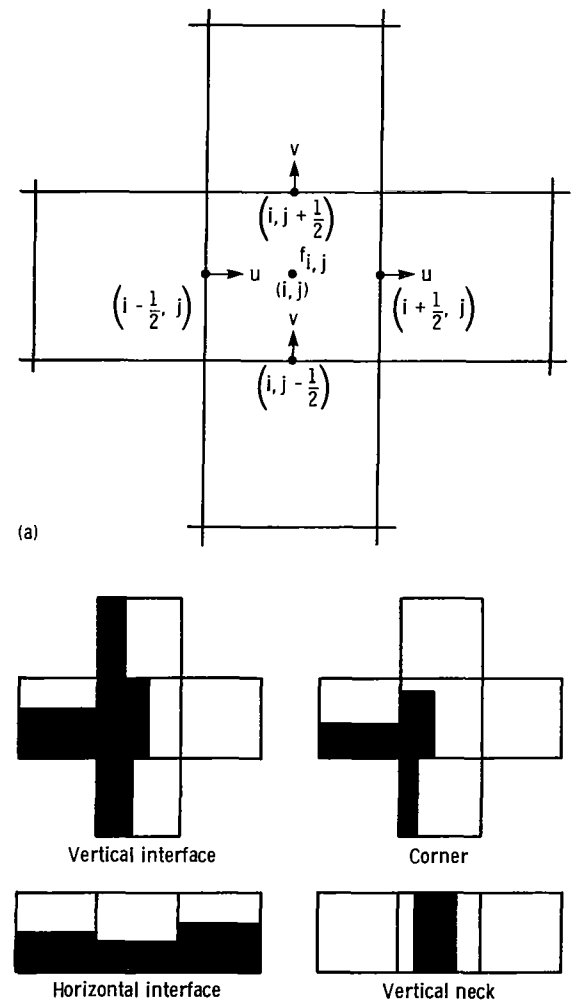

(a) Velocity components.
(b) Interface geometries.

Figure 6. - Computational elements for flame advection.

burning speed S_u in all possible directions of propagation instead of the advection velocity. Since the direction of propagation of the flame due to combustion is not known apriori, S_u is given all possible directions and the actual flame motion corresponding to all of the directions is calculated. Thus the flame speed is taken as

$$S_f = (S_u \cos \theta_i, S_u \sin \theta_i) \tag{17}$$

where

$$\theta_i = \frac{(i-1)\pi}{4}$$

and

$$i = 1,2, \ldots, 8$$

According to Huygen's principle, the actual flame propagation is the maximum advancement in all directions. Thus f can be updated as

$$f(t+\Delta t) = \underset{0 \le i \le 8}{\text{Max}}\, f^i \tag{18}$$

where

$$f^0 = f(t)$$

Combustion exothermicity. – Figure 7 explains the dynamic effect of burning due to the increase in specific volume in which a particle moves away from the flame front a distance of $2u_s$ after burning. To account for this effect in the two-dimensional calculations of the velocity field, changes in f due to flame advancement in the combustion step Δf_c are used to calculate the strength of the volumetric sources according to

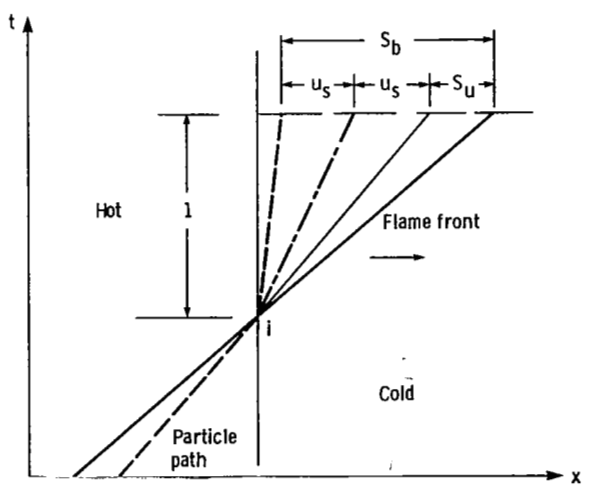

Figure 7. - Kinematics of flame front.

$$\Delta = 0.5(\nu - 1)h_c^2 \frac{\Delta f_c}{\Delta t_c} \tag{19}$$

where ν is the specific volume ratio across the flame. For each cell with $\Delta f_c > \Delta f_{\min}$, where $\Delta f_{\min}$ is a negligible change in volume, a source blob is generated and placed at the center of this cell. The core size of this blob is

$$r_0 = \frac{\Delta}{2\pi u_s} \tag{20}$$

where $u_s = 0.5(\nu - 1)S_u$ is the maximum velocity generated by the flame propagation.

Choice of Numerical Parameters

In choosing the input parameters to the computations, a compromise is made between the accuracy of the results and the efficiency of the computations in terms of time and storage.

To limit the number of vortex elements produced and subsequently used in the computations, the following values are recommended:

$$h = 0.2 \tag{21}$$

$$\Gamma_{\min} = 0.05 \tag{22}$$

This value of $\Gamma_{\min}$ results in the generation of four sheets in the first time step. Thus it provides a reasonable accuracy in calculating of the diffusion of these sheets into the field. Since the error of the method is expected to be $O(\Delta t)$ (ref. 3), the time step for the nonreacting flow is taken as

$$\Delta t = 0.1 \tag{23}$$

In the combustion calculations a cell size

$$h_c = 0.05 \tag{24}$$

was found appropriate to achieve a fine resolution of the flame front. Note that, since the flame surface is located within the cell, the resolution of the flame surface is not limited by h_c. The combustion time step must satisfy the Courant condition

$$\Delta t \le \frac{h_c}{2(u_{\max} + S_u)} \tag{25}$$

to keep the calculations stable. In most cases, $\Delta t_c < \Delta t$, and several combustion steps are performed for each vortex step by choosing $\Delta t = K\ \Delta t_c$, where K is an integer.

The Program

Figure 8 depicts the overall flow chart of the MIMOC program. For the sake of simplicity, only the major steps and subroutines are shown. The program listing contains an extensive array of comments and variable definitions to further explain it in detail. There are no input data for the program. All of the necessary parameters of the flow field are initialized in MIMOC; those for the walls are calculated in WLPNTS. If combustion computations are to be performed, subroutine INTCMB is called to initialize the combustion parameters such as the burning speed and the density ratio across the flame. If these parameters are changed, the program must be recompiled. The thick solid lines indicate that the control is in MIMOC. The thin solid lines identify the control with either of the two subroutines BOUNDR or COMBUS. The double box signifies the role subroutine POTVEL plays in the center of the calculations in the code.

At each time step, $t = t + \Delta t$, subroutine BOUNDR is called four times, one for each wall in the channel. BOUNDR acts like a master program for the application of the no-slip boundary condition along solid walls. To accomplish that, it starts by calling POTVEL to calculate the velocity on the wall due to the interior field. Subroutine SHEETS is called to calculate the velocity of vortex sheets and the velocity at the wall by using subroutine SHEVEL. If the net velocity at the wall is larger than a minimum, vortex sheets are generated or removed. SHEETS is also used to move the existing vortex sheets by using the velocity produced by the interior field as well as their induced velocity. Finally, BOUNDR calls SHEBLB to check the position of the vortex sheets and to transform those that leave the sheet layer into vortex blobs. Subroutines NRMWL2 and PRLWL2 are used to transform the coordinates of vortex sheets from wall coordinates to physical coordinates when they become vortex blobs. These blobs are fed immediately to POTVEL to account properly for their induced field, as indicated by the short-dashed line.

The control goes back to MIMOC after the calculations at the boundaries are finished. The position of the vortex blobs is updated by moving them according to their induced velocity and by random walk. MIMOC acts also as a sorter for vortex blobs in order to assign those near boundaries to the proper sheet layer. Vortex blobs that leave the interior zone are assigned back to SHEETS, as indicated by the long-dashed line, after their coordinates are adjusted in either NRMWL1 OR PRLWL1.

Subroutine COMBUS acts as a master program for the computations of flame propagation. First FLAME is called to move the flame by combustion. Here the normal burning speed S_u is used, and subroutine XNOH is called

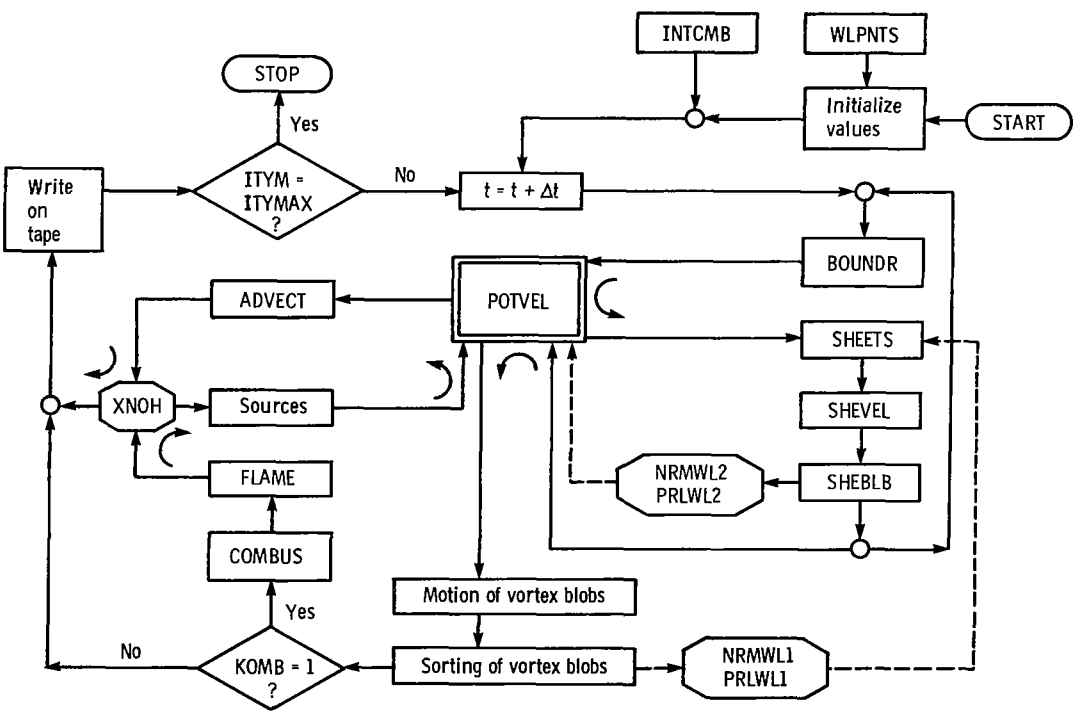

Figure 8. - Flow chart of the MIMOC main program.

to locate and move the interface inside each cell. This motion is employed in COMBUS to calculate the strength of the volumetric sources. COMBUS calls POTVEL to calculate the advection velocity at the center of the cells and uses it to calculate the velocity on the sides of these cells. This velocity is used in subroutine ADVECT to move the flame by calling XNOH for each cell. In MIMOC the results are written on a permanent file for later use and the time is updated again.

Results

Samples of the results obtained by using the program are shown in figures 9 to 12. The samples involve the vorticity field, the average velocity field, the turbulent statistics, the flame front geometry, and the concentration contours in a combustion channel with a rearward-facing step. (Similar results, computed for a free jet by using a modified version of the program, are presented in ref. 19.) The graphical outputs of the vorticity field and the flame front interface were plotted by employing computer graphics on a 16-mm black-and-white motion picture film. The concentration contours were displayed on a color image processor by assigning a relationship between color and the value of f and were recorded on color motion picture film. Examples of the output are provided in the motion picture supplement (C-308) of this report.

The computational time required to run this code can be long, as much as 4 to 5 hours on an IBM 370. As the number of vortex blobs increases, the running time per computational step grows as $O(N_V^2)$. However, in confined flows, such as the one considered in this report, N_V remains approximately constant. The number of vortex blobs used depends on the length of the vortex sheets h, the time step Δt, and the circulation of the vortex blobs Γ_{min}. The number of blobs determines the accuracy of the solution and the smallest scale of turbulence that can be resolved.

All of the computations were performed for a Reynolds number of 10 000. Presented in figure 9 is the vorticity field in flow over a rearward-facing step with an expansion ratio of 2. Figure 9(a) shows the development of the flow field by presenting vortex velocity vector fields that trace the motion of all of the vortex blobs included in the solution at successive dimensionless time intervals, each equal to 50 computational steps of 0.1. Figure 9(b) shows the growth of a large-scale eddy traced at time intervals equal to five computational steps. The formation of large-scale turbulent eddies, by the interaction of the incoming flow and the recirculating flow, can be readily seen in these results.

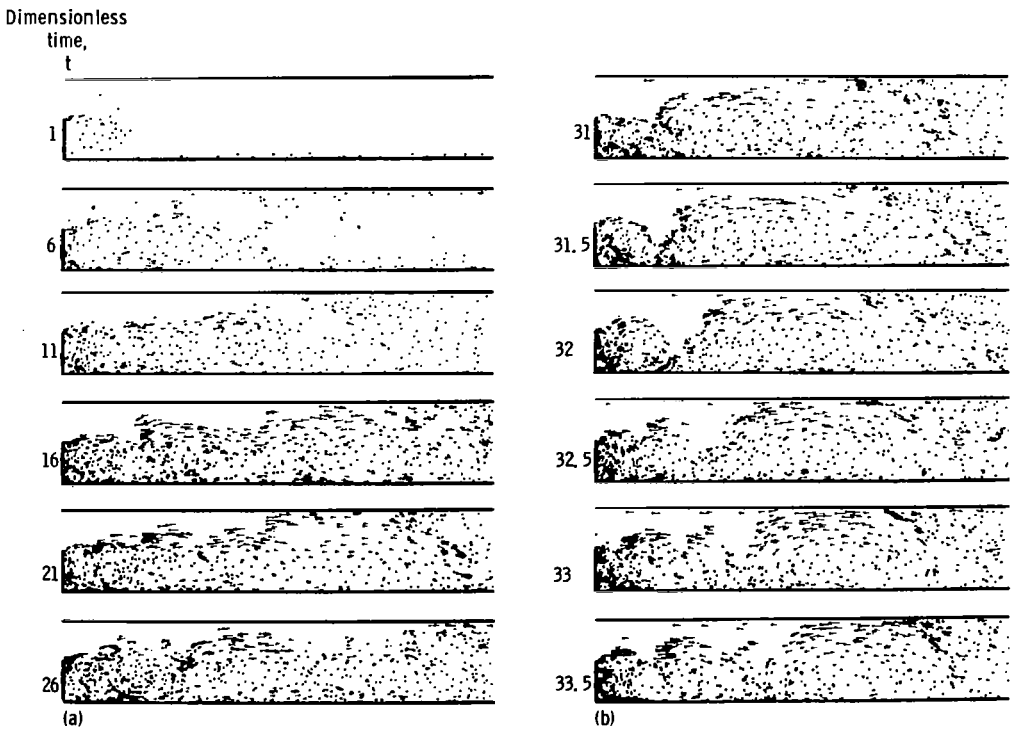

(a) Development of flow field.
(b) Growth of large-scale eddy.

Figure 9. - Vorticity field in channel with rearward-facing step. Expansion ratio, 2.

Figure 10 shows the average velocity profiles and the turbulent stress profiles in the same channel but with a smaller step (expansion ratio of 1.5). There are two sets of profiles for each variable. The set on the top corresponds to averaging between time steps 291 to 348, the set on the bottom, between time steps 158 to 200. The two sets resemble each other qualitatively although the top set is closer to steady-state conditions than the bottom set. This comparison shows that at least 300 steps are needed to build valid statistics. According to the average streamwise velocity profiles, shown in figure 10(a), the channel can be divided into three regions. The first region is dominated by the recirculation bubble with strong negative velocities. The second region starts at the reattachment zone with a boundary layer developing under a favorable pressure gradient. In the last region the two boundary layers, growing on both walls, converge to form the start of a fully developed flow in the channel. The average cross-stream velocity profiles are depicted in figure 10(b). Here the recirculation zone is marked by a positive value of this velocity component, but the rest of the channel is dominated by a negative vertical velocity that is due to the expansion of the flow to fill out the channel. The turbulent normal and turbulent shear stresses shown in figures 10(c) and (d), respectively, exhibit a maximum at the high shear zones, namely at the shear layer downstream from the step and in the boundary layers on both walls.

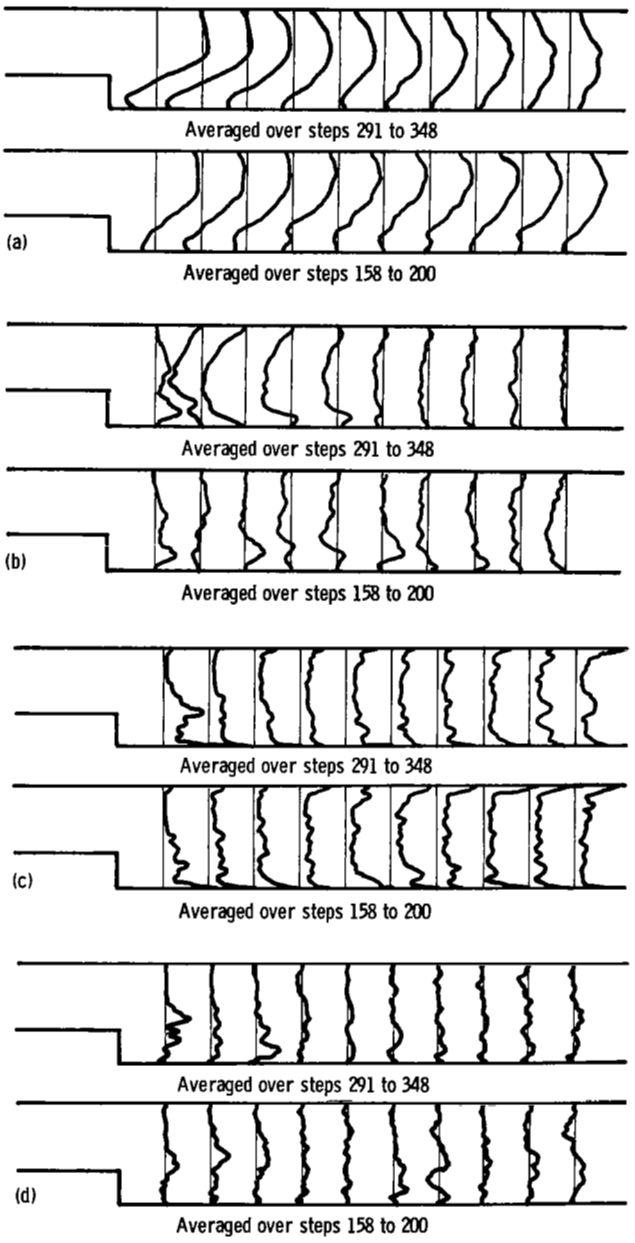

(a) Axial velocity.
(b) Cross-stream velocity.
(c) Turbulent normal stress $\overline{u'^2}$.
(d) Turbulent shear stress $-\overline{u'v'}$.

Figure 10. - Velocity profiles and turbulent statistics profiles. Reynolds number, 10 000; expansion ratio, 1.5.

Figure 11 displays the variation in the vorticity field and the flame front contour, shown as a demarcation line between cells with $f=0$ and those with $f>0$, calculated for a channel with an expansion ratio of 2, $S_u=0.02$, and $\nu=4$. These data correspond to a propane-air mixture burning at an equivalence ratio of 0.5. The figure consists of two sequential series of computer outputs. The sequence in figure 11(a) displays the process of ignition in the turbulent flow of figure 9 in a cell located on the centerline of the channel at a distance from the step equal to the height of the step. The sequence in figure 11(b) depicts the "stationary state" operation reached at $t=26.1$ after ignition at the bottom corner at the moment when the medium was set in motion. The number of computational time steps, $\Delta t=0.05$ each, between the solutions displayed here is 40 for figure 11(a) and 4 for figure 11(b). From these figures it can be concluded that the flame stabilizes itself on the outer edge of the large-scale eddies of the turbulent field and establishes an acceleration that reduces the length of the recirculation zone from that of a flow without combustion. These observations agree with the results of experiments by Ganji and Sawyer (ref. 20) and Pitz and Daily (ref. 21) in a similar channel with equivalent flow condition.

A black-and-white image of a color photograph of the flow described above is shown in figure 12. The numerical solution is displayed in figure 12(a) and the experimental record, in figure 12(b). The color of the numerical results was assigned according to the value of f, producing areas of constant concentration of products; the color of the experimental results changed with the gradient of the local temperature. In the black-and-white image, the bright areas, in both cases, represent the zones of maximum burning. The agreement between them is

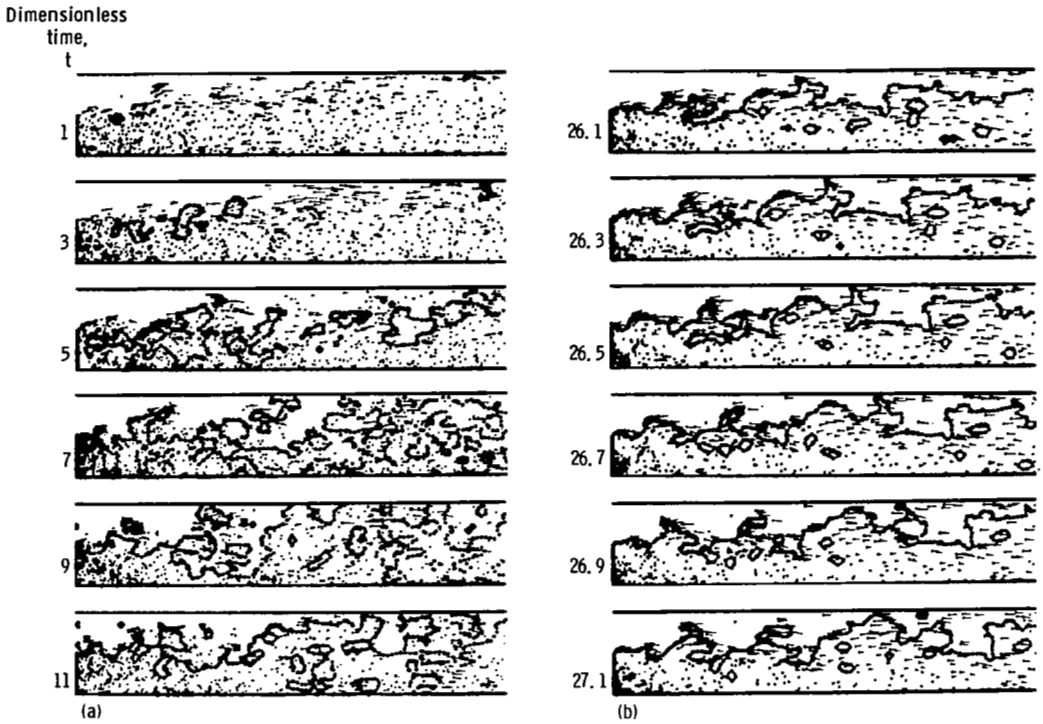

(a) Ignition in turbulent flow of figure 9 in cell located on centerline of channel at distance from step equal to step height.
(b) Stationary-state operation at t = 26.1 after ignition at bottom corner.

Figure 11. - Flame geometry and vorticity field with rearward-facing step. Reynolds number, 10 000; expansion ratio, 2.

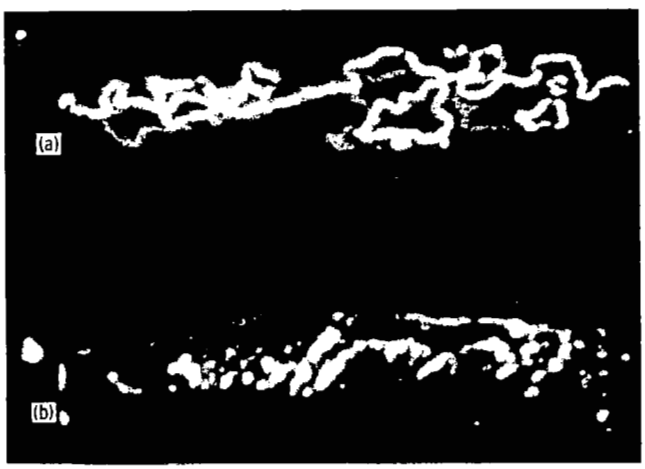

(a) Numerical. (b) Experimental.

Figure 12. - Concentration contours.

remarkable, considering the simplifications used to produce the numerical results. A 16-mm motion picture supplement (C-308) shows the dynamic nature of the calculation.

Conclusions

A computer code for calculating unsteady, two-dimensional turbulent reacting flow is presented in this report. The model used for the analysis is based on the random vortex method of computing the turbulent flow field. Because the method is grid free and devoid of numerical diffusion, it is suitable for modeling the intrinsic physical properties of flows at large Reynolds numbers. It can analyze large gradients produced by the small eddies of turbulent motion, and it allows perturbations to grow into possible instabilities without damping or undue dissipation. The combustion of premixed gases is idealized by the propagation of a flame interface, located between reactants and products, due to convection and self-propagation. The expansion of the flow across the flame due to the exothermicity of the reaction is taken into account by using a distribution of volumetric sources within the burning zone.

The program was used to study the flow field in a model combustor, formed by a rearward-facing step in a channel, in terms of the vorticity field, the velocity field, the turbulent shear stresses, the flame contours, and the concentration field. Results for the vorticity field reveal

the formation of large-scale eddy structures in the turbulent flow downstream from the step. Not only do these structures persist in the reacting case, but also the flame front almost surrounds the vorticity field and thus produces a situation in which the flame propagates along a streamline instead of normal to it. The process of stabilizing a turbulent flame behind a bluff body is illustrated by igniting a fully developed turbulent flow. The formation of a recirculation zone behind the step provides a continuous source of ignition by enhancing the contact between the products and the reactants. In addition, combustion is shown to reduce the length of the recirculation zone. The concentration field contours indicate that most burning occurs around the outer edges of the large eddies of the shear layer and that the combustion process extends far downstream in the channel.

National Aeronautics and Space Administration
Lewis Research Center
Cleveland, Ohio, March 28, 1983

Appendix – Routines in Computer Program

The 27 routines in the order that they appear in the computer program are listed here.

Vorticity Field Routines

MIMOC	main routine, initializes variables and directs program
BOUNDR	controls program flow to satisfy no-slip conditions at the walls
CFSCZ	differential transformation function
CRK4	Runge-Kutta integration
INIPUT	starts integration procedure using ZXACT
NMTRM	numerical transformation using reference point
NRMWL1	transforms from physical coordinates to wall coordinates for vertical walls when a blob becomes a sheet
NRMWL2	transforms from wall coordinates to physical coordinates for vertical walls when a sheet becomes a blob
PLTFLM	plots graphs
PNTWAL	checks on wall point transformation
POTVEL	computes velocity in physical plane from points in complex plane
PRLWL1	same as NRMWL1 except for horizontal walls
PRLWL2	same as NRMWL2 except for horizontal walls
RANDNM	generates Gaussian distribution of random numbers
SHEBLB	transforms vortex sheets into blobs
SHEETS	adds or removes sheets to satisfy no-slip boundary condition
SHEVEL	calculates sheet velocity
TRNSPP	transforms point by using a reference point
WLPNTS	sets values of wall points where boundary conditions will be checked
ZXACT	performs exact transformation from complex plane to physical plane

Combustion Routines

ADVECT	advances flame by advection
COMBUS	controls program flow for combustion
FLAME	advances flame by laminar flame speed
INTCMB	initializes combustion parameters
XNOH	moves individual flame interface
WD	generates uniform random numbers used by INTCMB and COMBUS
WDP	same as WD but completely independent

References

1. Ghoniem, A. F.; Chorin, A. J.; and Oppenheim, A. K.: Numerical Modeling of Turbulent Combustion in Premixed Gases. 18th Symposium (International) on Combustion, The Combustion Institute, 1981, pp. 1375–1383.
2. Ghoniem, A. F.; Chorin, A. J.; and Oppenheim, A. K.: Numerical Modeling of Turbulent Flow in a Combustion Tunnel. Phil. Tran. R. Soc. London Ser. A, vol. 304, 1982, pp. 303–325.
3. Chorin, A. J.: Numerical Study of Slightly Viscous Flow. J. Fluid Mech., vol. 57, pt. 4, 1973, pp. 785–796.
4. Chorin, A. J.: Flame Advection and Propagation Algorithm. J. Comp. Phys., vol. 35, 1980, pp. 1–11.
5. Noh, W. T.; and Woodward, P.: SLIC, Simple Line Interface Calculations. International Conference on Numerical Methods in Fluid Dynamics, 5th, A. I. Vooren and P. J. Zandbergen, eds., Springer-Verlag, 1976, pp. 330–339.
6. Keller, J. O.; et al.: Mechanism of Instabilities in Turbulent Combustion Leading to Flash Back. AIAA J., vol. 20, no. 2, 1982, pp. 254–262.
7. Mellor, A. M.: Turbulent-Combustion Interaction Models for Practical High Intensity Combustor. 17th Symposium (International) on Combustion. The Combustion Institute, 1978, pp. 377–387.
8. Mellor, A. M.; and Ferguson, C. R.: Practical Problems in Turbulent Reacting Flows. Turbulent Reacting Flows, P. A. Libby and F. A. Williams, eds., Springer-Verlag, 1980, pp. 45–64.
9. Bray, K. N. C.: The Interaction Between Turbulence and Combustion. 17th Symposium (International) on Combustion, The Combustion Institute, 1978, pp. 223–233.
10. Bray, K. N. C.: Turbulent Flow with Premixed Reactants. Turbulent Reacting Flows, P. A. Libby and F. A. Williams, eds., Springer-Verlag, 1980, pp. 115–184.
11. Williams, F. A.: Combustion Theory. Addison-Wesley, 1965.
12. Libby, P. A.; and Williams, F. A.: Fundamental Aspects—Turbulent Reacting Flows. P. A. Libby and F. A. Williams, eds., Springer-Verlag, 1980, pp. 1–43.
13. Chorin, A. J.: Vortex Sheet Approximation of Boundary Layers. J. Comp. Phys., vol. 27, 1978, pp. 428–442.
14. Chorin, A. J.: Vortex Models and Boundary Layer Instabilities. SIAM J. Scientific Stat. Comp., vol. 1, no. 1, Mar. 1980, pp. 1–21.
15. Williams, F. A.: A Review of Some Theoretical Consideration of Turbulent Flame Structure, Analytical and Numerical Methods for Investigation of Flow Fields with Chemical Reactions, Especially Related to Combustion. M. Barrer, ed., AGARD CP 164, AGARD, 1975, pp. III–1 to III–25.
16. Batchelor, G. K.: An Introduction to Fluid Mechanics. Cambridge University Press, London, 1967.
17. Chorin, A. J.; and Marsden, J. E.: A Mathematical Introduction to Fluid Mechanics. Springer-Verlag, 1979.
18. Ghoniem, A. F.; and Oppenheim, A. K.: Random Element Method for the Numerical Modeling of Diffusional Processes. Presented at the 8th International Conference on Numerical Methods in Fluid Dynamics (Aachen, West Germany), June 28–July 2, 1982.
19. Ghoniem, A. F.; Chen, D. Y.; and Oppenheim, A. K.: Formation and Inflammation of a Turbulent Jet. Presented at the Spring Technical Meeting of the Combustion Institute, Canadian Sec. (Banff, Alberta, Canada), May 9, 1982.
20. Ganji, A. R.; and Sawyer, R. F.: An Experimental Study of the Flowfield of a Two-Dimensional Premixed Turbulent Flame. AIAA J., vol. 18, no. 7, July 1980, pp. 817–824.
21. Pitz, R. W.; and Daily, J. W.: Experimental Study of Combustion in a Turbulent Free Shear Layer Formed at a Rearward Facing Step. AIAA Paper 81-0106, Jan. 1981.

Lewis motion-picture film supplement C-308 is available on loan. Requests will be filled in the order received.

The film (16 mm, 15 min, color, sound) shows high-speed color schlieren motion pictures of a premixed propane-air flame stabilized by a rearward-facing step. A numerical technique that uses a random walk method for turbulence modeling and does not rely on empirical closure models was developed for analyzing turbulent combustion. Computer-produced color motion pictures of the volume fraction burned are used to compare the predictions with the experimental records.

Requests for film supplement C-308 should to be addressed to

NASA Lewis Research Center
Attn: Chief, Management Services Division (60-1)
21000 Brookpark Road
Cleveland, OH 44135

cut

Date _____

Please send, on loan, copy of film supplement C-308 to TP-2132

Name of Organization

Street Number

City and State Zip Code

Attention: Mr. _____

Title _____

1. Report No.	2. Government Accession No.	3. Recipient's Catalog No.
NASA TP-2132		

4. Title and Subtitle	5. Report Date
MODELING INTERFACE MOTION OF COMBUSTION (MIMOC) - A COMPUTER CODE FOR TWO-DIMENSIONAL, UNSTEADY TURBULENT COMBUSTION	August 1983
	6. Performing Organization Code 505-32-32
7. Author(s)	8. Performing Organization Report No.
Ahmed F. Ghoniem, Cecil J. Marek, and Antoni K. Oppenheim	E-1569
	10. Work Unit No.
9. Performing Organization Name and Address	11. Contract or Grant No.
National Aeronautics and Space Administration Lewis Research Center Cleveland, Ohio 44135	
	13. Type of Report and Period Covered
12. Sponsoring Agency Name and Address	Technical Paper
National Aeronautics and Space Administration Washington, D. C. 20546	14. Sponsoring Agency Code

15. Supplementary Notes Ahmed F. Ghoniem, University of California, Berkeley (work done under NASA grant NAG3-131); Cecil J. Marek, Lewis Research Center; Antoni K. Oppenheim, University of California, Berkeley (work done under NASA grant NAG3-131). Film supplement C-308 available on request. Program available from COSMIC, University of Georgia, Athens, Ga. 30602.

16. Abstract

A computer code for calculating the flow field and flame propagation in a turbulent combustion tunnel is described. The model used in the analysis is the random vortex model of Chorin, which allows the turbulent field to evolve as a fundamental solution of the Navier-Stokes equations without averaging or closure modeling. The program was used to study the flow field in a model combustor, formed by a rearward-facing step in a channel, in terms of the vorticity field, the turbulent shear stresses, the flame contours, and the concentration field. Results for the vorticity field reveal the formation of large-scale eddy structures in the turbulent flow downstream from the step. The concentration field contours indicate that most burning occurred around the outer edges of the large eddies of the shear layer.

17. Key Words (Suggested by Author(s))	18. Distribution Statement
Turbulence Vorticity Flame Computer code	Unclassified - unlimited STAR Category 07

19. Security Classif. (of this report)	20. Security Classif. (of this page)	21. No. of Pages	22. Price*
Unclassified	Unclassified	18	A02

* For sale by the National Technical Information Service, Springfield, Virginia 22161 NASA-Langley, 1983